

DYNAMIC ANALYSIS OF DARRIEUS VERTICAL AXIS WIND TURBINE COMPOSITE BLADES

¹SOBHY GHONEAM, ²AHMED HAMADA, ³TAHA SHERIF

^{1,2,3}Faculty of Engineering, Menoufia University, Menoufia, Egypt

E-mail: ¹Ghoneam22000@yahoo.com, ²a_ahmed_59@yahoo.com, ³tahasherif12@yahoo.com

Abstract - This paper gives a numerical and experimental investigation of the dynamic analysis of Darrieus vertical axis wind turbine (D-VAWT) which is suitable for countries have a moderate wind speed. The wind turbine performance can be improved using composite material blades. Also, corrosion and wear problems can be treated using light wind turbine blades manufactured from composite laminates. The lamination plate theory is utilized to compute the laminate extension, bending and coupling stiffness for each composite blade. Based on wind turbine design parameters, the Darrieus rotor- type vertical axis wind turbine models (D-VAWTs), aerodynamic characteristics (blade speed ratio (ϕ) and coefficient of power (C_p)) and dynamic characteristics (natural frequencies and mode shapes) are presented. The mathematical finite element models (FEM) are developed to compute the dynamic-nature for composite blades. Modified mechanical parameters are introduced to improve the reliability and accuracy of the developed models. As well as, this paper seeks to enhance investigation of numerical and experimental results through using a suitable experimental small prototypes of darrieusvertical axis wind turbine blades. The dynamic responses such as: frequency, mode shape and damping factor were extensively investigated using FFT analyzer.

Keywords - H-Darrieus Wind Turbine – Aerodynamic Characteristics - Composite Materials – Finite Element Analysis – Modal Testing.

I. INTRODUCTION

Among renewable energy sources, wind energy generation may be considered as the most rapidly growing form of electrical power generation in the world because it is one of the most cost-effective and environmentally friendly. Wind turbines can be classified mainly into two types: Horizontal-Axis Wind Turbines (HAWTs) and Vertical-Axis Wind Turbines (VAWTs). VAWTs have several advantages over HAWTs: The generator, gearbox, and so forth can be placed on the ground, and a tower may not be required for the machine operation. This leads to much easier servicing, a VAWT does not have to be pointed toward the wind. Also, there is no need for a yaw mechanism to turn the rotor against the wind because a Vertical axis wind turbine (VAWT) captures energy irrespective of the direction of the wind in the horizontal plane. VAWTs are preferred for applications requiring small-scale standalone wind turbines [1], [2].

There are two types of VAWTs: lift (Darrieus) and drag (Savonius). Darrieus wind turbines have a higher cut-in wind speed than Savonius wind turbines [3]. In this study, H-Darrieus (straight-bladed) wind turbines are investigated. The previous advantages of Darrieus wind turbines have made them the focus of many studies.

A review of various Darrieus VAWT configurations and its performance is introduced in [3]-[5]. A complete design methodology of a straight-bladed vertical axis wind turbine blade is introduced in [6]. Conceptual design of a large-scale floating offshore vertical axis turbine [7]. The effects of design factors on mechanical performances of Vertical Axis Wind Turbines (VAWTs) were investigated in [8]. The

effects of a blade profile, the Reynolds number, and the solidity on the performance of a straight-bladed vertical axis wind turbine are investigated in [9]. Effect of pitch angle on power performance and aerodynamics of a vertical axis wind turbine [10]. Pitch Optimization in Small-size Darrieus Wind Turbines is explained in [11]. Investigation of Effect of Cambered Blades on Darrieus VAWTs [12]. An experimental and numerical analysis of the start-up behavior of a three-bladed H – Darrieus VAWT is discussed in [13]. Leading-edge serrations for performance improvement on a vertical-axis wind turbine at low tip-speed-ratios [14]. Measurements of power coefficient as a function of tip speed ratio (C_p (ϕ)) are presented in [15]. The effect of using composite VAWT blades is presented in [16]. A numerical and experimental comparison between the structural behavior of a wind generator with straight blades and a composite prototype of a wind generator with helical blades is presented in [17].

The aim of the present paper is to investigate the dynamic analysis of composite material blades and its effect on the whole wind turbine performance. Six configurations of straight-bladed VAWT composite blades are designed, simulated and fabricated of Glass – Polyester with different stacking sequence for each. The lamination plate theory is utilized to compute the laminate extension, bending and coupling stiffness for each composite blade. The equivalent property method is utilized to obtain the mechanical properties of each stacking composite blade. The mathematical finite element models (FEM) are developed to compute the dynamic-nature for wind turbine composite blades. Several numerical modal analysis studies in SolidWorks simulation 2019 software are utilized to investigate the effect of

different stacking sequences and blade number on the dynamic behavior of the blade. Experimental modal analysis is carried out using B & K data acquisition type (3160-A-042) analyzer equipped with Pulse 17.1 software to get the dynamic characteristics of the composite blade.

II. DESIGN OF MODELS

In this section, the main design parameters of H – Darrieus VAWT are introduced.

A. No. of blades (n)

The choice of blade number is a compromise between the blade stiffness, aerodynamic efficiency and also cost considerations [7]. Three designed models with 2, 3 and 4blade number are established to verify the effect of blade number on the turbine's performance.

B. Blade speed ratio (ϕ)

$$\phi = \omega R / V \quad (1)$$

Where, ω is the angular speed of the turbine rotor, R is the radius of the wind turbine and V is the wind speed (m/s).

C. Solidity (σ)

According to [6], [9], Power production can be increased by increasing the value of solidity but at the same time, the developed torque on the blade increases. The range of solidity is taken as 0.25 – 0.5 for the three designed models. The solidity is defined as the ratio of blade area with rotor area and presented as;

$$\sigma = nc/D \quad (2)$$

Where, D is the diameter of the turbine and c is the chord length.

D. Aspect ratio (AR)

High values of aspect ratio are recommended for straight bladed VAWTs [18]. The aspect ratio is introduced as follows;

$$AR = H/c \quad (3)$$

Where, H is the blade length.

E. Blade profile

According to [6], [9], For straight bladed VAWT, NACA 00xx series of symmetric airfoils are more frequently used because the high-digit NACA00xx airfoil provides higher power in a low speed zone. In this study, the NACA0015 airfoil is chosen as the blade profile for designated wind turbine blades.

F. Input wind energy (P_w)

The input energy (P_w) of wind passes through a turbine presented in [19], [20] as follows;

$$P_w = 0.5 \rho AV^3 \quad (4)$$

Where, ρ is air density (1.225 Kg/m³) and A is the blade swept area ($A = 2RH = D^2$)

G. Power coefficient (C_p)

According to [9], [20], the power coefficient (C_p) is obtained as the ratio between the output rotor power (P_B) and the input wind energy as follows;

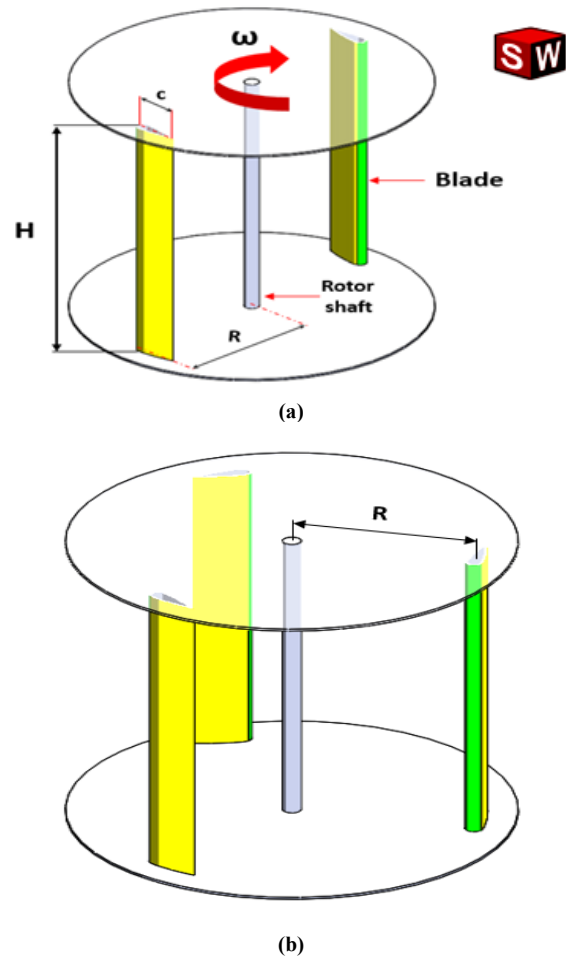
$$C_p = \frac{P_B}{P_w} = \frac{T\omega}{0.5 \rho AV^3} \quad (5)$$

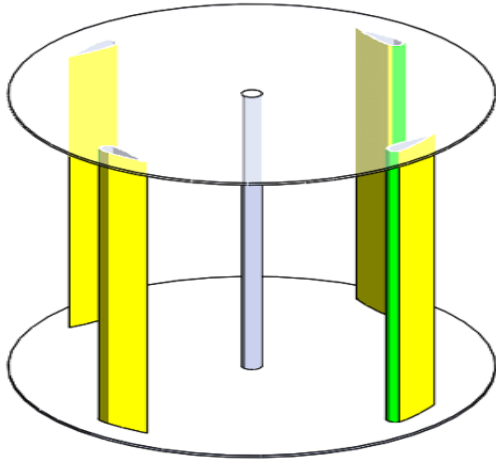
Where, T is the rotor torque (N.m).

H-Darrieus prototypes with either two, three and four straight blades are designed according to the previous formulas, its main characteristics are reported in Table I and shown in Fig. 1.

Model characteristics	Two – bladed Model	Three – bladed Model	Four – bladed Model
Diameter (D)=Height (H)	64cm	64cm	64cm
Chord length, c	8cm	8cm	8cm
Aspect ratio, AR _{blade}	8	8	8
Blade thickness, t	4mm	4mm	4mm
Solidity, σ	0.25	0.375	0.5
Coefficient of power, C_p	0.22	0.24	0.21

Table I. Main characteristics of the three designed models





(c)
Fig. 1. Features and dimensions of (a) Two – bladed model, (b) Three – bladed model and (c) Four – bladed model

III. MATERIAL PREPARATION AND PROPERTIES

A vertical axis wind turbine blade must have certain useful material properties. The most important of these properties are adequately high yield strength for longer life, high material stiffness to maintain optimal aerodynamic performance and low density for reduced amount of gravity and normal force component. The modern wind turbine materials are composites made up of fiberglass reinforcements. The blade made up of composite materials can have thin walls due to high strength to weight ratio of the

materials. For turbine blade design, they are composed of E-glass with epoxy, polyester or vinyl ester and normally hand-layup fabrication techniques are used [7], [16].

In the current search, six configurations of composite blades are produced of glass – polyester. Each blade was made of six layers with various stacking sequence for each as: set1:[0°/90°/0°/90°/0°/90°], set2:[0°/90°/0°/90°/R/R], set3:[0°/90°/R/R/0°/90°], set4:[R/R/0°/90°/R/R], set5:[R/R/R/0°/90°] and set6:[R/R/R/R/R/R].

Where, R:Random, 0°:Unidirectional and 90°:Ninety angle oriented fibers.

A sample of Stacking sequence for a composite blade is shown in Fig. 2.

The utilized Composite Material (discontinuous random short fibers, resin, continuous fiber) is composed of Standard E-Glass, random fiber and polyester with catalyst addition as matrix. These properties are indicated in Table II.

According to [21]-[23], The tensile strength (σ_{ult}), Young's modulus (E), Poisson's ratio (ν_{xy}), and the composite blade density (ρ) are calculated analytically according to mixture rule and specific theoretical equations and their results are listed in Table III.

Properties	Materials		
	Polyester Resin	Glass Fiber	Random Fiber
Modulus of elasticity, E (GPa)	3.5	72.4	9.17
Density, ρ (Kg/m ³)	1260	2530	2540
Poisson's ratio, ν_{xy}	0.35	0.22	0.21

Table II. Material properties of resin and reinforcement fiber of composite blade.

No.	Code number	σ_{ult} (GPa)	E (GPa)	ν_{xy}	ρ (Kg/m ³)
I	[0°/90°/0°/90°/0°/90°]	2.08	44.84	0.27	2028
II	[0°/90°/0°/90°/R ₂]	1.44	32.94	0.27	2028
III	[0°/90°/R ₂ /0°/90°]	1.38	28.12	0.27	2028
IV	[R ₂ /0°/90°/R ₂]	0.89	19.55	0.27	2028
V	[R ₄ /0°/90°]	0.83	15.47	0.27	2028
VI	[R ₆]	0.43	6.40	0.27	2028

Table III. Results of mechanical properties of stacked composite blades.

IV. NUMERICAL MODAL ANALYSIS

This section discusses the modal analyses performed numerically on the six-different blade stacking sequences and the whole H – Darrieus VAWT structure. The responses are in the frequency domain obtained numerically by means of the Finite Element models using SOLIDWORKS Simulation 2019 software [24].

A. Models constraints and loadings

Aiming at characterizing and comparing the mechanical behavior of the three straight-bladed Darrieus VAWTs and in order to simulate the inertial loads associated to the turbine rotation and to the weight of the structures, the following constraint and boundary conditions are applied to the structures.

Cylindrical surface constraints are applied on the lower and upper edges of the rotor shaft as shown in Fig. 3.

The computed composite material properties of each composite blade configuration is entered into the SOLIDWORKS Material library as a new material. Stacking sequence properties of each composite blade configuration is applied to the simulated model. Moreover, the acceleration of gravity is imposed along the z-axis. All the boundary conditions, mesh and loading of the three-bladed model are shown in Fig. 3.

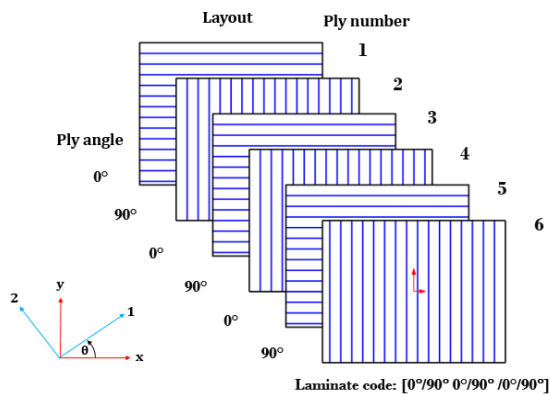


Fig.2. Stacking sequence of a composite blade.

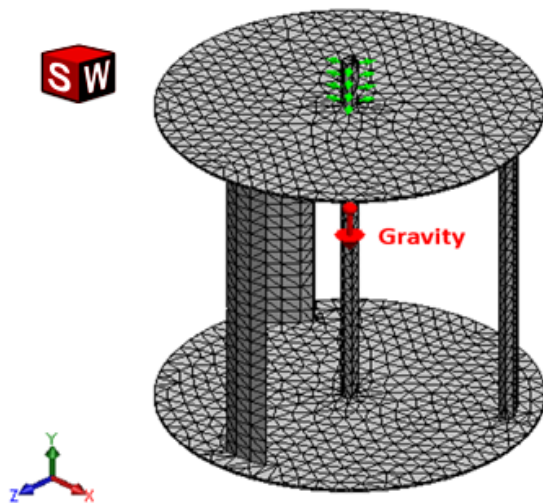


Fig. 3. Model constraints and loading for three – bladed model.

B. Numerical modal results

Under the mentioned constraints and loadings, the numerical frequency analysis was run. The modal results computed for three designed models are listed in Table IV.

These results show that the modal frequencies related to the straight composite blade are high, thus highlighting the stiffer behavior introduced by the use of composite materials. Moreover, this behavior increases the gap between the first natural frequency

and operative frequency range of the turbine that spans the interval 0–5 Hz.

V. EXPERIMENTAL MODAL ANALYSIS

This section shows the experimental setup and results obtained from experimental modal tests conducted on local manufactured experimental prototypes.

The experimental set up is schematically shown in Fig.4. The experimental set-up consists of the wind tunnel, Darrieus wind rotor, and measurement devices. The wind tunnel used in the experiments is an open-circuit type with the power capacity of 5 kW and has a circular exit. The Darrieus wind rotor and measurement devices have been installed away from the exit of this wind tunnel. The Darrieus rotor and measurement devices have been placed on a steel profile frame. The Darrieus rotor shaft has been supported near the top and bottom by a very low friction ball bearing to minimize the friction force. And then measurements of rotor torque, wind velocity and the number of revolution have been measured by a torque gauge sensor, anemometer and a laser revolution counter (laser tachometer). The torque gauge sensor and a revolution counter (tachometer) have been coupled to the upper part of the rotor.

A digital torque transducer unit connecting MTT03-12 torque gauge sensor with a measuring range of 0–135 N.cm has been used to measure the torque that forms on Darrieus wind rotor shaft and the accuracy of torque meter sensor is $\pm 0.5\%$. A laser tachometer of type GTC-TA110 is utilized to count the rotor revolutions with a range of (+1)–(+99,999) rpm and the accuracy of laser tachometer equipment is $\pm 0.02\%$.

Both the response of the wind rotor and the excitation signal were measured and connected to a B&K data acquisition type (3160-A-042) analyzer equipped with B&K pulse 17.1 software used for the analysis and conditioning of the signals.

Analyzer in conjunction with the Fast Fourier Transform (FFT) gives the mathematical relationship between time and frequency successively and displays the frequency response spectrum (FRS) in addition to registering the coherence functions with the desired frequency range [25].

The resulted responses were registered by a piezoelectric accelerometer type (4506) its weight 18 gram mounted at the bearing. As well as the accelerometer signals were conditioned in the charge amplifier in order to feed dual channel analyzer.

A PC equipped with the software is connected to the multi-channel signal analyzer, which is used to collect, analyze and display the signals, Frequency Response Function (FRF) is automatically calculated and graphically presented through the software. Modal parameters are extracted from the FRF for

each wind turbine configuration. For each test 5 impulses acceleration time histories responses are acquired in order to compute averaged Frequency Response Functions (FRFs).

Dynamic analysis is presented to investigate dynamic Eigen parameters including natural frequencies,

torque and critical speed of the three experimental prototypes shown in Fig. 5. Eigen frequencies which must be considered through rotation of turbines are listed in Table V.

Code number	Two – bladed Model			Three – bladed Model			Four – bladed Model		
	Mode 1	Mode 2	Mode 3	Mode 1	Mode 2	Mode 3	Mode 1	Mode 2	Mode 3
[0°/90°/0°/90°/0°/90°]	928.71	1014.4	1353.3	950.97	1267.6	1303.6	899.29	1588.7	1630.4
[0°/90°/0°/90°/R ₂]	795.99	869.42	1159.9	815.07	1086.5	1117.3	770.78	1361.7	1397.4
[0°/90°/R ₂ /0°/90°]	735.46	803.29	1071.7	753.08	1003.9	1032.3	712.15	1258.1	1291.2
[R ₂ /0°/90°/R ₂]	613.23	669.79	893.55	627.92	837.02	860.78	593.8	1049	1076.6
[R ₄ /0°/90°]	545.50	595.82	794.86	558.57	744.57	765.71	528.22	933.18	957.67
[R ₆]	350.86	383.23	511.25	359.27	478.91	492.5	339.75	600.22	615.97

Table IV. Numerical results of the first three natural frequencies of three designed models (rad/s).

Code number	Two – bladed Model		Three – bladed Model		Four – bladed Model	
	ω_1	ζ_1	ω_1	ζ_1	ω_1	ζ_1
[0°/90°/0°/90°/0°/90°]	945	0.16	973	0.10	912	0.06
[0°/90°/0°/90°/R ₂]	821	0.19	830	0.13	785	0.09
[0°/90°/R ₂ /0°/90°]	750	0.23	765	0.18	725	0.13
[R ₂ /0°/90°/R ₂]	632	0.28	637	0.21	603	0.15
[R ₄ /0°/90°]	557	0.34	570	0.25	535	0.19
[R ₆]	360	0.36	368	0.28	345	0.22

TableV. Values of Fundamental Natural Frequency (rad/s) and Damping Factor for three experimental models..

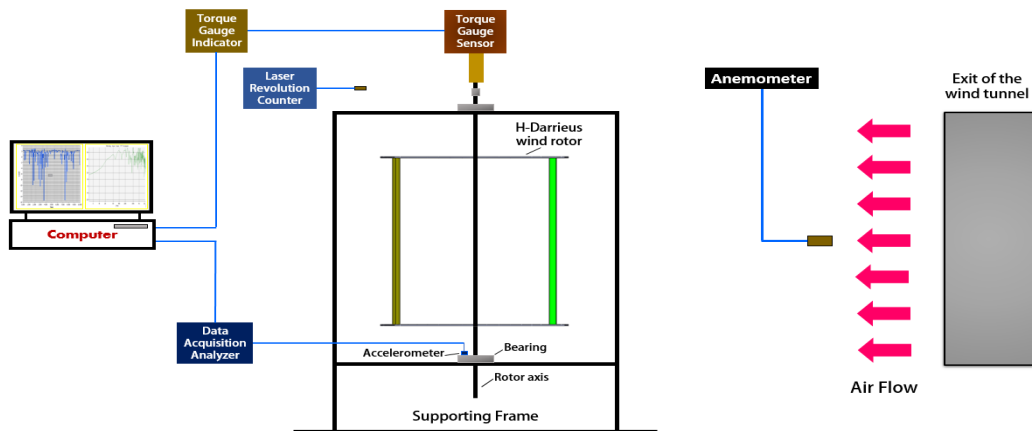


Fig. 4. Schematic diagram of experimental system.



(a)



(b)



Fig. 5. Experimental test rig of (a) Two – bladed model, (b) Three – bladed model and (c) Four – bladed model.

VI. RESULTS AND DISCUSSION

From results of mechanical properties of six composite blade configurations as shown in Table III, It can be noticed that the tensile strength and Young's modulus of composite blades configuration $[R_6]$ are lower than those of other blades, and blades configuration $[0^\circ/90^\circ/0^\circ/90^\circ/0^\circ/90^\circ]$ have higher ones. This is due to the fibers are aligned in the direction of the longitudinal elasticity and consequently are able to store their energy, while the random fiber assist to dissipated energy. In the composite blade, the resonance frequencies of the specimens have been recorded and analyzed for different stacking sequence. The computed and measured fundamental natural frequencies are given in Table IV and Table V. As expected the frequencies of blades configuration $[R_6]$ are lower than those of other configurations, and code number: $[0^\circ/90^\circ/0^\circ/90^\circ/0^\circ/90^\circ]$ have higher ones.

The magnitude of natural frequencies in the configuration $[0^\circ/90^\circ/0^\circ/90^\circ/0^\circ/90^\circ]$ are 2.65 times greater than those in code number: $[R_6]$. The changing of the fiber stacking sequence of the composite blade from $[0^\circ/90^\circ/0^\circ/90^\circ/0^\circ/90^\circ]$ to $[R_6]$ decreases natural frequencies as shown in Fig. 6 (a).

Regarding the damping values, Table V. shows that the configuration with $[R_6]$ has high damping values compared with the $[0^\circ/90^\circ/0^\circ/90^\circ/0^\circ/90^\circ]$ due to high dissipated energy. It is observed that the damping factor is small for code number $[0^\circ/90^\circ/0^\circ/90^\circ/0^\circ/90^\circ]$ compared with the other code numbers as shown in Fig.6 (b). This is explained by the fact that fiber orientations in these directions are expected to increase the blade stiffness and result in less energy dissipation.

For random blade configuration $[R_6]$, the damping factor is high compared with the other orientations. The direction of short fiber decreases the blade stiffness, where the maximum energy dissipation results in a large system damping factor.

Determination of the natural frequencies and mode shapes of a vibrating composite blade is an important

aspect from the stand point of view of the structure dynamic behavior. The natural frequency gives information about resonance avoidance for certain loading conditions. Mode shape, on the other hand, gives indication about the vibration level at each position of the blade. One of the most important parameters from designer's point of view is the location of nodes and antinodes. The nodes are the positions at which the vibration vanishes, the maximum stresses induced at these nodes. While the antinodes are the positions at which maximum vibration level occurs.

From Table IV, it is shown that the modal frequencies related to the composite blade are high, thus highlighting the stiffer behavior introduced by the use of composite materials. Moreover, this behavior increases the gap between the first natural frequency and operative frequency range of the turbine that spans the interval 0–5 Hz. Fig. 7 shows mode shape for first three modes of tested three -bladed model. The three- bladed model is noticed to have the higher fundamental natural frequency leading to more stable behavior over operating conditions than the other designed models.

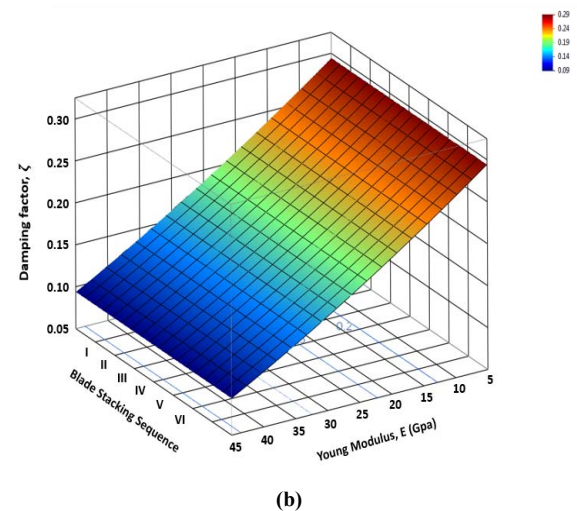
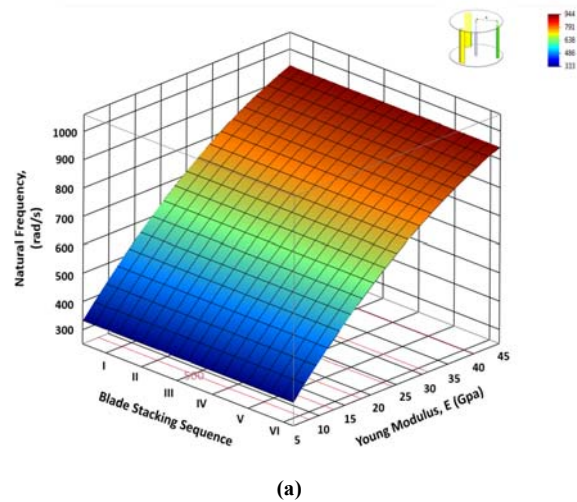


Fig. 6. (a) Fundamental Frequency and (b) associated damping factor response surface for six composite blade configurations of the three-bladed model.

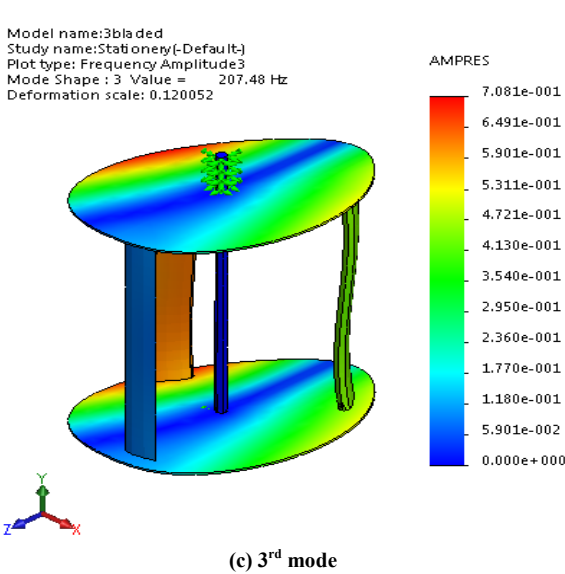
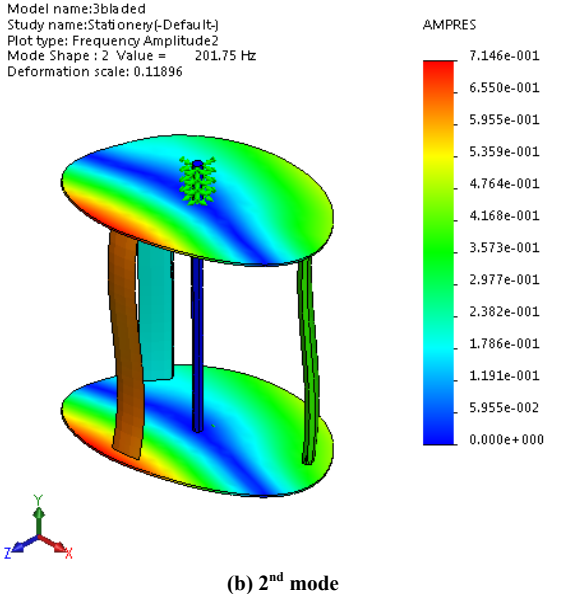
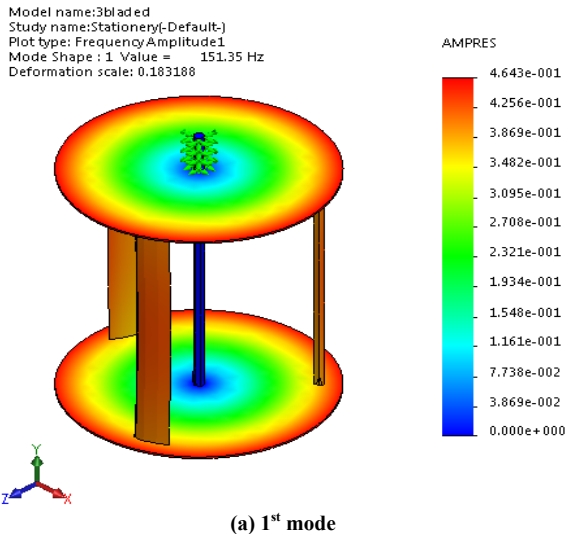


Fig. 7. Modal shapes of the three-bladed model.

VII. CONCLUSION

From the numerical and experimental results, the following concluding points can be drawn:

1. For the fabricated glass fiber/polyester composite blades, the blade stacking sequence configuration [0/90/0/90/0/90], the tensile strength, Young's modulus (E), major Poisson's ratio (ν_{xy}), are higher than those of the other types of composite including [0/90/0/90/R₂], [0/90/R₂/0/90], [R₂/0/90/R₂], [R₄/0/90], and random glass fiber/polyester composite blades, [R₆].
2. The present comparison between the numerical and experimental results proves that the suggested finite element models of the composite blades provide an efficient tool for the dynamic analysis with proper accuracy.
3. The mutual influences of anisotropy, stacking sequence, and vibration mode are significant on the damping capacity.
4. With the proper choice of stacking sequence, fiber and matrix materials for the composite blades, high values of system damping factor for various modes of composite blades may be obtained.
5. The three-bladed model is noticed to have the higher fundamental natural frequency leading to more stable behavior over operating conditions than the other designed models

Finally, this study is useful for the designer in order to select the lamina stacking sequence, to shift the natural frequencies as desired or to control the vibration level.

REFERENCE

- [1] MOHD. HASAN ALI, "WIND ENERGY SYSTEMS, Solutions for Power Quality and Stabilization," CRC Press Taylor & Francis Group, pp. 1-35, 2012.
- [2] Pramod Jain, "Wind Energy Engineering," The McGraw-Hill Companies, Inc, pp. 9-50, 2011.
- [3] Willy Tjiu, TjukupMarnoto, Sohif Mat, MohdHafidz Ruslan and KamaruzzamanSopian, "Darrieus vertical axis wind turbine for power generation I: Assessment of Darrieus VAWT configurations," Renewable Energy, Elsevier, vol. 75, pp. 50-67, 2015.
- [4] Muhammad Mahmood Aslam Bhutta, Nasir Hayat, Ahmed Uzair Farooq, Zain Ali, Sh. Rehan Jamil and Zahid Hussain, "Vertical axis wind turbine – A review of various configurations and design techniques," Renewable and Sustainable Energy Reviews vol. 16, pp. 1926–1939, 2012.
- [5] Xin Jin, Gaoyuan Zhao, KeJun Gao and Wenbin Ju, "Darrieus vertical axis wind turbine: Basic research methods," Renewable and Sustainable Energy Reviews, Elsevier, vol. 42, pp. 212–225, 2015.
- [6] M. Saqib Hameed and S. Kamran Afaq, "Design and analysis of a straight bladed vertical axis wind turbine blade using analytical and numerical techniques," Ocean Engineering, Elsevier, vol. 57, pp. 248–255, 2013.

- [7] Brian Hand, Andrew Cashman, "Conceptual design of a large-scale floating offshore vertical axis wind turbine," *Energy Procedia* by Elsevier Ltd, vol.142, pp. 83-88, 2017.
- [8] Chaianant Sranpat, Suchaya Unsakul, Premchai Choljararux, Thananchai Leephakpreeda, "CFD-based Performance Analysis on Design Factors of Vertical Axis Wind Turbines at Low Wind Speeds," *Energy Procedia*, vol. 138, pp. 500-505, 2017.
- [9] Sung-Cheoul Roh and Seung-Hee Kang, "Effects of a blade profile, the Reynolds number, and the solidity on the performance of a straight bladed vertical axis wind turbine," *Journal of Mechanical Science and Technology* vol. 27, pp. 3299-3307, 2013.
- [10] Abdolrahim Rezaeiha, Ivo Kalkman, Bert Blocken, "Effect of pitch angle on power performance and aerodynamics of a vertical axis wind turbine," *Applied Energy* by Elsevier Ltd, vol. 197, pp. 132-150, 2017.
- [11] Alessandro Bianchini, Lorenzo Ferrari and Lorenzo Ferrari, "Pitch Optimization in Small-size Darrieus Wind Turbines," 69th conference of the Italian Thermal Machines Engineering Association, ATI2014, *Energy Procedia*, vol. 81, pp. 122-132, 2015.
- [12] Sayyad Basim Qamara and Isam Janajreh, "Investigation of Effect of Cambered Blades on Darrieus VAWTs," *Energy Procedia* by Elsevier Ltd, vol. 105, pp. 537 – 543, 2017.
- [13] Alessandro Bianchini, Lorenzo Ferrari and Sandro Magnani, "START-UP BEHAVIOR OF A THREE-BLADED H-DARRIEUS VAWT: EXPERIMENTAL AND NUMERICAL ANALYSIS," *Proceedings of ASME Turbo Expo*, 2011.
- [14] Zhenyu Wang, Yuchen Wang and Mei Zhuang, "Improvement of the aerodynamic performance of vertical axis wind turbines with leading-edge serrations and helical blades using CFD and Taguchi method," *Energy Conversion and Management* by Elsevier Ltd, vol. 177, pp. 107-121, 2018.
- [15] J. Kjellin, F. Bülow, S. Eriksson, P. Deglaire, M. Leijon and H. Bernhoff, "Power coefficient measurement on a 12 kW straight bladed vertical axis wind turbine," *Renewable Energy*, Elsevier, vol. 36, pp. 3050-3053, 2011.
- [16] M. Saqib Hameed, S. Kamran Afaq and Farzeen Shahid, "Finite Element Analysis of a Composite VAWT Blade," *Ocean Engineering*, Elsevier, vol. 109, pp. 669-676, 2015.
- [17] Andrea Alaimo, Francesco Lo Iacono, Giacomo Navarra, Giovanni Pipitone, "Numerical and experimental comparison between two different blade configurations of a wind generator," *Composite Structures*, vol. 136, pp. 526-537, 2016.
- [18] Islam, Mazharul, Fartaj, Amir, Carriveau, Rupp, "Analysis of the design parameters related to a fixed-pitch straight-bladed vertical axis wind turbine," *Wind Eng.* vol. 32 (5), pp. 491-507, 2008.
- [19] P. Schubel and R. Crossley, "wind turbine blade design," *Journal of energies*, vol. 5, pp. 3425 – 3449, 2012.
- [20] Okeoghene Eboibi, Louis Angelo M. Danao, Robert J. Howell, "Experimental investigation of the influence of solidity on the performance and flow field aerodynamics of vertical axis wind turbines at low Reynolds numbers," *Renewable Energy*, vol. 92, pp. 474 – 483, 2016.
- [21] Chou, Tsu-Wei, Kelly, Anthony, "Mechanical properties of composites," *Annu. Rev. Mater. Sci.* vol. 10, pp. 229-59, 1980.
- [22] M. A. Elkhier, A. A. Hamada, A. B. Eldeen, "Prediction of fatigue life of glass reinforced polyester composite using modal testing", *International Journal of Fatigue* 69, pp. 28-35, 2014.
- [23] P.K. Mallick, "FIBER REINFORCED COMPOSITES Materials, Manufacturing, and Design," by Taylor & Francis Group, LLC, 2008.
- [24] Paul Kurowski, "Vibration Analysis with SolidWorks Simulation 2019," SDC publications, 2019.
- [25] A. Maher, A. A. Hamada, "Dynamic analysis of laminated composite structure with bolted joints," 8th International Conference on production engineering and control, PEDAC, 2004

★ ★ ★